Author Manuscript

Author Manuscript

Author Manuscript

Author Manuscript

HHS Public Access

Author manuscript

Ann Biomed Eng. Author manuscript; available in PMC 2018 November 01.

Published in final edited form as:

Ann Biomed Eng. 2017 November ; 45(11): 2626–2634. doi:10.1007/s10439-017-1891-8.

The Quantitative Structural and Compositional Analyses of Degenerating Intervertebral Discs using Magnetic Resonance Imaging and Contrast-Enhanced Micro-Computed Tomography

Kevin H. Lin[1] and **Simon Y. Tang**[2,3,4]

[1]Biology, Washington University, St. Louis, MO

[2]Biomedical Engineering, Washington University, St. Louis, MO

[3]Mechanical Engineering and Materials Science, Washington University, St. Louis, MO

[4]Orthopaedic Surgery, Washington University, St. Louis, MO

Abstract

The intervertebral disc (IVD) is susceptible to degenerative changes that are associated with low back pain. Murine models are often used to investigate the mechanistic changes in the development, aging, and diseased states of the IVD, yet the detection of early degenerative changes in structure is challenging because of the minute size of the murine IVDs. Histology is the gold standard for examining the IVD structure, but it is susceptible to sectioning artifacts, spatial biases, and requires the destructive preparation of the sample. We have previously demonstrated the feasibility of using Ioversol for the contrast-enhanced micro-computed tomography (microCT) to visualize and quantitate the intact healthy murine IVD. In this work, we demonstrate utility of this approach to monitor the longitudinal changes of *in vitro* nucleolytic- and mechanical injury-degeneration models of the murine discs and introduce novel quantitative metrics to characterize the structure and composition of the IVD. Moreover, we compared the imaging quality and quantitation of these *in vitro* models to magnetic resonance imaging (MRI) and histology. Stab puncture, trypsin injection, and collagenase injection all induced detectable and significant changes in structure and composition of the discs overtime. Compared to MRI and histology, contrast-enhanced microCT produced superior images that capture the degenerative progression in these models. Contrast-enhanced microCT was also capable of monitoring the structural deteriorations via the changes in disc heights and volumes, and the nucleus pulposus intensity/disc intensity (NI/DI) parameter provides a surrogate measure of proteoglycan composition ($R = 0.96$). Overall, this approach allows for the nondestructive monitoring of the structure and composition of the IVD at very high resolutions.

Keywords

Intervertebral disc; Contrast-enhanced MicroCT; MRI; Disc Degeneration; Ioversol; Proteoglycans; Nucleus pulposus

Corresponding Author: Simon Y. Tang, Ph.D., Assistant Professor, Department of Orthopaedic Surgery, Musculoskeletal Research Center, Washington University, St Louis MO, 660 South Euclid Ave, Box 8233, St. Louis, MO 63110, tangs@wudosis.wustl.edu, Phone: (314) 286-2664, Fax: (314) 362-0334.

Author Manuscript Author Manuscript Author Manuscript Author Manuscript

Introduction

Degeneration of the intervertebral disc (IVD) is associated with low back pain [1,2] and the hallmarks of the degenerative process involves the loss of structural integrity and biochemical alterations including the loss of proteoglycans [2–4], as well as a number of cellular and physiological changes [5,6]. The IVD is a prominent symphysis in the spine, and it consists of a gelatinous nucleus pulposus (NP) bounded by the concentrically lamellar annulus fibrosus (AF) [7]. The degeneration of the IVD typically initiates with the gradual loss of proteoglycans in the NP, followed by a reduction in disc height, and ultimately resulting in collapse of the IVD. The degeneration of the IVD impedes the IVD's ability to transmit loads and may impair mobility and spinal range of motion [8].

The clinical evaluation of the IVD in humans typically relies on Magnetic Resonance Imaging (MRI), which provides a structural assessment of the tissue as well as some surrogate compositional measures of the IVD [9–11]. MRI operates through the detection of hydrogen atom vibration in response to an oscillating magnetic field, and it is particularly suited for the imaging of hydrated tissues such as the IVD [12,13]. Specialized pulse sequences such as the T2 can resolve the structural components of the IVD including the AF and the NP [14]. T2 relaxation mapping additionally allows the surrogate measurement of composition [15]. Although MRI is useful for animals studies of the IVD [16], the spatial resolution of MRI for small animal models may limit its ability to accurately detect nuanced changes. We have previously demonstrated a novel contrast-enhanced micro-computed tomography (microCT) technique that allows for the high-resolution, noninvasive imaging of the rat and mouse IVDs with greater accuracy and precision than histology [17]. To determine the ability of this technique to monitor IVD degeneration, we propose to apply this approach to monitor the cascade in several established IVD degeneration models: puncturing of the IVD, injection of trypsin, and injection of collagenase. The puncture of the IVD using a needle mimics a mechanical injury by physically breaching the IVD [18,19]. Trypsin is a serine protease that catalyzes the hydrolysis of peptide bonds, and previous studies showed that trypsin injection into the NP deteriorates IVD mechanical behavior and GAGs content [20,21]. Collagenase is a particularly harsh degeneration method and degrades both the collagen-rich AF as well as the NP [22]. Moreover, these chemical agents have been shown to induce structural changes of the IVD and therefore helpful tools to induce controlled degradation of the IVD in order to validate imaging modalities [23].

These degeneration models will be assessed by high-resolution MRI and histology in order to compare the contrast-enhanced microCT technique against the two gold standards of IVD imaging. In addition to the 3D morphology, we also introduce a novel parameter, the ratio of nucleus pulposus intensity to disc intensity (NI/DI), which provides an indicator of the proteoglycan composition within the IVD. Taken together, we show here that contrast-enhanced microCT can provide detailed nondestructive, longitudinal monitoring of structural and compositional changes in several *ex vivo* degenerative models of the murine IVD at high resolutions.

Author Manuscript Author Manuscript Author Manuscript Author Manuscript

Methods

Dissection of Rat FSUs and models of degeneration

Fifty-eight rat functional spinal units (FSUs), consisting of an intervertebral disc sandwiched by the intact endplate and vertebrae on both sides, were dissected from the tails of 4-month old Sprague Dawley rats. The FSUs were randomly distributed into four groups: control (n=12), stab (n=18), trypsin (n=18), and collagenase (n=10). Control samples were kept intact, while the stab, trypsin, and collagenase samples were injected with phosphate buffered saline (PBS), 0.05% trypsin (Sigma 59417C), and 0.2% collagenase (equal concentrations of collagenase I and II, Sigma C0130 and C6885) respectively immediately following the 0 day time point. Seven days was selected to be the terminal time point in order to assess the ability of the different imaging modalities to resolve the early degenerative changes within the IVD.

Contrast-enhanced MicroCT

Samples designated for longitudinal microCT were incubated in a solution of 50 mg/mL Ioversol solution diluted from a stock of OptiRay 350 (Guerbet, St. Louis) in PBS supplemented with 1% penicillin-streptomycin at 37C one day prior to the day 0 timepoint. At the 0, 2, 5, and 7 day timepoints, samples were removed from incubation and then scanned using a VivaCT40 (Scanco Medical, CH) at 10 μm voxel size (45kVp, 177uA, high resolution, 300ms integration). The sample is immediately returned to 37C in the respective treatment condition after each scan.

Following our previous method for segmentation of murine IVDs [17], the microCT data is exported as a DICOM file for further processing. Following an initial median filter (sigma = 0.8, support = 3), bone is then thresholded out, and the soft tissue not part of the IVD was removed by drawing contours around the outer edge of every 5 transverse slices of the AF and morphed using a linear interpolation. The remaining voxels are designated as the whole disc mask. To generate a mask of the NP, a histogram of the annuation values of the disc is used to generate a threshold mask. This mask then undergoes a morphological close followed by a morphological open to remove rough edges and fill interior holes to become the final NP mask. From the masks of the whole disc and the NP, volumes and average attenuations (intensity) are calculated. The volume is determined from the total number of voxels contained within the mask and the attenuation is taken as the average 16-bit grayscale value of the voxels.

Disc heights and visualizations of the microCT were obtained using OsiriX (Pixmeo, Geneva). The disc height represents the average disc height across five evenly spaced points along the mid-sagittal plane of the IVD.

1,9 Dimethylmethylene Blue

The proteoglycan composition was directly measured from the control, the stab-, and the trypsin-degenerated samples using a calibrated 1,9-dimethylmethylene blue (DMMB) (Sigma 341088) assay. Following a microCT scan, each sample was digested in papain solution (0.8 mg / 100 mg tissue) overnight. 1,9-DMMB was used to assay s-GAG content

Author Manuscript Author Manuscript Author Manuscript Author Manuscript

of the digested sample with chondroitin sulfate as standard. The proteoglycan content assessed by the DMMB assay is compared to the ratio of nucleus pulposus intensity/disc intensity (NI/DI), the average attenuation of voxels in the previously described NP and whole disc masks, which represents a normalized measure of the NP attenuation.

Magnetic Resonance Imaging (MRI)

MRI was conducted with an Agilent 4.7T small animal imaging system (Agilent Technologies, Santa Clara, CA) using an in-house, custom 1 cm ID solenoid coil. Sagittal 3D multi-echo gradient echo images were acquired at 100 μm^3 isotropic resolution using the following parameters: TR= 50 ms, TE=1.52 ms, echo spacing = 5 ms, flip angle = 30 degrees, 10 averages, 4 minute 16 second acquisition. The images were manually segmented using custom MATLAB software. T2 relaxation measurements were performed using 3D multi-echo spin echo images were acquired at 200 μm^3 isotropic resolution using the following parameters: TR = 1000 ms, TE = 6.65 ms, echo spacing 6.65 ms, 1 average, 34 minute acquisition. The T2 relaxation time measurements were made by performing a mono-exponential fit of the spin echo MRI data, and the mean and standard deviations of the resultant T2 were determined from the relaxation time constants across all the entire sample.

Histology

Samples designated for histology were incubated in PBS supplemented with 1% penicillin-streptomycin at 37C a day prior to the 0-day time point and then treated with the corresponding treatments. At the 0, 2, 5, and 7 day timepoints, samples were removed from the incubation solution and then fixed for 2 days in 10% neutral buffered formalin followed by 5 days of decalcification in Immunocal (StatLab 1414-X). The samples were embedded in paraffin, sectioned at a thickness of 10μm, and then stained with Safranin-O and Fast Green.

Statistical analyses

Two-way ANOVA and the General Linear Model were used to determine the effects of treatment, incubation times, and their interactive effects on microCT-measured disc height, whole disc volume loss, and whole disc attenuation loss. The Tukey's LSD post-hoc analyses was used to compare specific differences between these groups. T2 relaxation times were compared using the Chi-square test to examine the distributions between samples compared with the control. Pearson's correlation was used to determine the relationship between NI/DI and proteoglycan content of the IVDs. Effects and groups were considered statistically different when the $p < 0.05$. The statistics were done using Prism 6.0h (GraphPad, San Diego, CA).

Results

The quantitation of the disc structure using disc height, whole disc volume loss, and whole disc attenuation loss revealed significant longitudinal changes in the IVDs due to treatment conditions (Figure 2). The control group maintained its disc height and volume over time (Fig 2A, 2B), but the whole disc attenuation declined progressively over the incubation period (Fig 2C). The stab-injury group exhibited a significant loss of disc height at day 7

Author Manuscript Author Manuscript Author Manuscript Author Manuscript

(Fig 2A), and exhibited significant decline of disc volumes compared to the controls at day 5 and day 7 (Fig 2B). The stab-injury group also showed a more rapid decline in attenuation by day 2 that resulted in a significant declines at day 7 compared to control 7-day and stab 0-day (Fig 2C). Trypsin did not cause significant changes in disc height (Fig 2A), and a significant change in volume only after 7 days of incubation (Fig 2B). However, trypsin significantly reduced the whole disc attenuation at day 2 and day 7 (Fig 2C). Finally, the collagenase eroded the disc structure with dramatic and significant losses of disc height, disc volume, and whole disc attenuation. The disc structure in all of the collagenase-treated samples disintegrated by day 7 which resulted in the inability to conduct analyses on these samples.

A subset of control, stabbed, and trypsin treated samples were also assessed by the DMMB assay immediately after contrast-enhanced microCT scanning. The NI/DI was computed for these samples, and NI/DI showed a significant and strong correlation with the percent proteoglycan content (Fig 3; $p < 0.001$; $R=0.9581$; Bland-Altman correlation [24,25]). These results suggest that microCT imaging has the ability to accurately quantify relative amounts of proteoglycans in the IVD. It was not possible to segment the NP from the AF in the collagenase treated samples due to lack of differential contrast as a result of the rapid degeneration and thus NI/DI was not quantified for these samples.

Images from the contrast-enhanced microCT revealed visually striking progressions of the degeneration models over time (Figure 4). The border of the AF and the NP remain distinct in the control group throughout the incubation period despite some losses of attenuation. Both the trypsin- and stab-degenerative models exhibit a loss of demarcation between the AF and NP compartments, with the trypsin- group qualitatively showing a greater loss. The collagenase treated groups confirmed the significant quantitative losses of disc height, and whole disc volume and attenuation. It was not possible to distinguish the AF from the NP in the collagenase samples.

Histology of these samples revealed similar findings as the microCT visualization (Figure 5). Stab- and trypsin- degenerative models both showed reduce uptake of safranin-O that suggest a reduction in proteoglycans across all time points. Consistent with the microCT findings, the collagenase treated groups resulted in the dramatic collapse of the IVD structure with no safranin-O staining confirming the loss of the disc structures. Unlike the microCT data, the histological samples are cross-sectional rather than longitudinal, and therefore each panel reflects a different sample.

The T2-weighted MR images show the disc with more granular resolution compared to microCT (Fig 6A). The T2 relaxation times confirm a loss of hydration due to the trypsin- and stab- degradation (Fig 6B). Transverse views of the segmented disc images show a loss of disc height in the degenerative samples (Fig 6C).

Discussion

Diagnosing intervertebral disc degeneration in early stages using minimally invasive imaging techniques is important for understanding disease pathology and developing

Author Manuscript Author Manuscript Author Manuscript Author Manuscript

therapeutic strategies [9,26,27]. Contrast-enhanced microCT utilizing Ioversol is able to obtain detailed qualitative observations and precise quantitative measurements of the IVD structure longitudinally in several *ex vivo* degeneration models. The changes in disc morphology is captured through in three-dimensions, and this enables the ability to visualize the changes and obtain structural and compositional data at a nominal isotropic voxel size of 10 μms. With recent advances in CT technology, the voxel sizes can be as small as 700 nm. Since histological sections are on the order of 6–15 μm with the inevitable loss of tissue in serial sections, this microCT approach here may provide a more complete picture of the tissue of interest with a greater degree of accuracy. Although histological approaches remain powerful for determining molecular localization [28,29], structural analyses using contrast-enhanced microCT will be more accurate.

Three dimensional imaging modalities including the microCT and MRI can remove the influence of bias due to the selection of sectioning planes that are common in histology. The ability to nondestructively image the sample also enables the subsequent histological analyses and other assays of the same sample. Previous studies have shown success in utilizing T2 MRI to monitor the rat tail *in vivo* [30,31], and in the current study we found that it was indeed feasible to monitor the disc using MRI. The resolution of the MRI however introduces substantial uncertainties in quantifying the structure of the disc. In particular, features such as the NP appear as only a few voxels, and this introduces substantial uncertainties in quantitation. Moreover, the use of custom coils can introduce substantial edge artifacts particularly across ill-defined interfaces such as in the collagenase-treated samples[32]. The microCT resolution deployed here is 10 μm×10 μm×10 μm resulting in voxels that are 1,000 μm^3, while the MRI resolution is 100 μm×100 μm×100 μm resulting in 1,000,000μm^3 voxels. Utilization of contrast-enhanced microCT thus achieves resolutions three orders of magnitude better than MRI. MRI offers the advantage of enabling longitudinal in vivo studies, but MRI may not detect early degenerative changes due to its resolution. It is worth noting that we have previously shown that this contrast-enhanced microCT technique is compatible with live organ culture, however the *in vivo* utility remains to be investigated.

The microCT data also revealed changes in the disc shape when comparing control, stab, and trypsin treated samples across the timepoints, while the collagenase samples resulted in such dramatic changes that quantitation was not always possible in this group. Although the control samples also exhibited some degree of loss in structure and attenuation, which is expected for a devitalized sample incubating at a physiological temperature for 7 days, the stab and trypsin treated samples nevertheless degraded more than the control group, showing sharp drops in attenuation in the NP indicated by the transitions from higher attenuation (yellow) to lower attenuation (red). These changes are consistent with our expectations as the discs treated by stab and trypsin are known to show loss of proteoglycans in the NP, with trypsin showing greater losses [18–21]. The stabbing of the mouse IVD may have produced an injury that is disproportionally large compared to the size of the IVD and this resulted in significant degeneration compared to larger rodents that receive mechanical stab. Although collagenase treatment results in severe degeneration and may not be physiologically relevant [22], this treatment allows us to create a spectrum of degeneration and evaluate the effectiveness of each imaging modalities in monitoring varying degrees of degeneration.

Author Manuscript Author Manuscript Author Manuscript Author Manuscript

There are a number of limitations in this study. By design, this study does not account for the cellular level effects that may occur with trypsin or the stab, although both are shown to produce structural and inflammatory changes[19–21,33,34]. Further, the microCT-derived intensity attenuation values of the NP require regional normalization to either the AF in order to compute meaningful values of NI/DI. By normalizing for these geometric and compositional variations within IVDs, it is possible to provide nondestructive surrogate measurements for the DMMB assay. This imaging technique also allows for the nondestructive and repeated measurement of the same sample over time, providing a significant benefit in understanding the adaptive changes that occur with the initiation and progression of disc degeneration. Finally, due to sample dimension limitations, we were not able to physically separate the each IVD into AF and NP compartments for the DMMB assay, and thus we were unable to directly confirm our findings whether trypsin-mediated reduction of PGs occurred in NP or AF. However, it is well-known that the NP is rich in PGs and the AF is low in PGs, and the DMMB measurements of the intact IVD will most likely reflect changes in the NP.

In summary, a high-resolution functional microCT imaging of the murine intervertebral disc was developed and validated using *ex vivo* models of degeneration. The technique described here may be widely applied to other soft tissues that have variations in tissue-level charge density such as articular cartilage and meniscus. This method can be used for monitoring the 3 dimensional structural changes of diseases and treatments of the intervertebral disc. Moreover, sophisticated modeling techniques could be applied to data obtained from high-resolution imaging to monitor degeneration and efficacy of therapies [35–38]. This hydrophilic contrast agent does not induce toxicity to the tissue [17,39], thus providing a promising *in vitro* [17,40] and *in vivo* approach to monitor soft tissue degeneration.

Acknowledgments

The authors gratefully acknowledge Dan Leib for technical assistance on the microCT analyses, and Dr. James Quirk for technical assistance on the MRI. The authors acknowledge the support from the Washington University Musculoskeletal Research Center NIH P30 AR057235, NIH K01AR069116, and NIH R21AR069804. The authors gratefully acknowledge the generous gift of OptiRay 350 from Guerbet Pharmaceuticals.

References

1. Luoma K, Riihimaki H, Luukkonen R, Raininko R, Viikari-Juntura E, Lamminen A. Low Back Pain in Relation to Lumbar Disc Degeneration. Spine (Phila Pa 1976). 2000; 25(4):487–492. DOI: 10.1097/00007632-200002150-00016 [PubMed: 10707396]
2. Antoniou J, Steffen T, Nelson F, et al. The human lumbar intervertebral disc: evidence for changes in the biosynthesis and denaturation of the extracellular matrix with growth, maturation, ageing, and degeneration. J Clin Invest. 1996; 98(4):996–1003. DOI: 10.1172/JCI118884 [PubMed: 8770872]
3. Hickey DS, Hukins DW. Relation between the structure of the annulus fibrosus and the function and failure of the intervertebral disc. Spine (Phila Pa 1976). 1980; 5(2):106–116. [PubMed: 6446156]
4. Duance VC, Crean JK, Sims TJ, et al. Changes in collagen cross-linking in degenerative disc disease and scoliosis. Spine (Phila Pa 1976). 1998; 23(23):2545–2551. [PubMed: 9854753]
5. Zhao C, Wang L, Jiang L, Dai L. The cell biology of intervertebral disc aging and degeneration. Ageing Res Rev. 2007; 6(3):247–261. DOI: 10.1016/j.arr.2007.08.001 [PubMed: 17870673]
6. Vo NV, Hartman RA, Yurube T, Jacobs LJ, Sowa GA, Kang JD. Expression and regulation of metalloproteinases and their inhibitors in intervertebral disc aging and degeneration. Spine J. 2013; 13(3):331–341. DOI: 10.1016/j.spinee.2012.02.027 [PubMed: 23369495]

Author Manuscript Author Manuscript Author Manuscript Author Manuscript

7. Marchand F, Ahmed AM. Investigation of the laminate structure of lumbar disc anulus fibrosus. Spine (Phila Pa 1976). 1990; 15(5):402–410. [Accessed November 4, 2015] http://www.ncbi.nlm.nih.gov/pubmed/2363068. [PubMed: 2363068]
8. Mimura M, Panjabi MM, Oxland TR, Crisco JJ, Yamamoto I, Vasavada A. Disc Degeneration Affects the Multidirectional Flexibility of the Lumbar Spine. Spine (Phila Pa 1976). 1994; 19(12) http://journals.lww.com/spinejournal/Fulltext/1994/06000/Disc_Degeneration_Affects_the_Multidirectional.11.aspx.
9. Mwale F, Iatridis JC, Antoniou J. Quantitative MRI as a diagnostic tool of intervertebral disc matrix composition and integrity. Eur Spine J. 2008; 17(Suppl 4):432–440. DOI: 10.1007/s00586-008-0744-4
10. Benneker LM, Heini PF, Anderson SE, Alini M, Ito K. Correlation of radiographic and MRI parameters to morphological and biochemical assessment of intervertebral disc degeneration. Eur Spine J. 2005; 14(1):27–35. DOI: 10.1007/s00586-004-0759-4 [PubMed: 15723249]
11. Urban JPG, Winlove CP. Pathophysiology of the intervertebral disc and the challenges for MRI. J Magn Reson Imaging. 2007; 25(2):419–432. DOI: 10.1002/jmri.20874 [PubMed: 17260404]
12. Jung BA, Weigel M. Spin echo magnetic resonance imaging. J Magn Reson Imaging. 2013; 37(4): 805–817. DOI: 10.1002/jmri.24068 [PubMed: 23526758]
13. Majumdar S. Magnetic resonance imaging and spectroscopy of the intervertebral disc. NMR Biomed. 2006; 19(7):894–903. DOI: 10.1002/nbm.1106 [PubMed: 17075964]
14. Welsch GH, Trattnig S, Paternostro-Sluga T, et al. Parametric T2 and T2* mapping techniques to visualize intervertebral disc degeneration in patients with low back pain: initial results on the clinical use of 3.0 Tesla MRI. Skeletal Radiol. 2011; 40(5):543–551. DOI: 10.1007/s00256-010-1036-8 [PubMed: 20878155]
15. Marinelli NL, Haughton VM, Munoz A, Anderson PA. T2 relaxation times of intervertebral disc tissue correlated with water content and proteoglycan content. Spine (Phila Pa 1976). 2009; 34(5): 520–524. DOI: 10.1097/BRS.0b013e318195dd44 [PubMed: 19247172]
16. Jazini E, Sharan AD, Morse LJ, et al. Alterations in T2 relaxation magnetic resonance imaging of the ovine intervertebral disc due to nonenzymatic glycation. Spine (Phila Pa 1976). 2012; 37(4):E209–15. DOI: 10.1097/BRS.0b013e31822ce81f [PubMed: 21857410]
17. Lin KH, Wu Q, Leib DJ, Tang SY. A novel technique for the contrast-enhanced microCT imaging of murine intervertebral discs. J Mech Behav Biomed Mater. 2016; 63:66–74. DOI: 10.1016/j.jmbbm.2016.06.003 [PubMed: 27341292]
18. Ulrich JA, Liebenberg EC, Thuillier DU, Lotz JC. ISSLS prize winner: repeated disc injury causes persistent inflammation. Spine (Phila Pa 1976). 2007; 32(25):2812–2819. DOI: 10.1097/BRS.0b013e31815b9850 [PubMed: 18246002]
19. Abraham AC, Liu JW, Tang SY. Longitudinal changes in the structure and inflammatory response of the intervertebral disc due to stab injury in a murine organ culture model. J Orthop Res. 2016; 34(8):1431–1438. DOI: 10.1002/jor.23325 [PubMed: 27273204]
20. Perie D, Iatridis JC, Demers CN, et al. Assessment of compressive modulus, hydraulic permeability and matrix content of trypsin-treated nucleus pulposus using quantitative MRI. J Biomech. 2006; 39(8):1392–1400. DOI: 10.1016/j.jbiomech.2005.04.015 [PubMed: 15970200]
21. Mwale F, Demers CN, Michalek AJ, et al. Evaluation of quantitative magnetic resonance imaging, biochemical and mechanical properties of trypsin-treated intervertebral discs under physiological compression loading. J Magn Reson Imaging. 2008; 27(3):563–573. DOI: 10.1002/jmri.21242 [PubMed: 18219615]
22. Bromley JW, Hirst JW, Osman M, Steinlauf P, Gennace RE, Stern H. Collagenase: an experimental study of intervertebral disc dissolution. Spine (Phila Pa 1976). 1980; 5(2):126–132. [PubMed: 6247767]
23. Antoniou J, Mwale F, Demers CN, et al. Quantitative magnetic resonance imaging of enzymatically induced degradation of the nucleus pulposus of intervertebral discs. Spine (Phila Pa 1976). 2006; 31(14):1547–1554. DOI: 10.1097/01.brs.0000221995.77177.9d [PubMed: 16778686]

Author Manuscript Author Manuscript Author Manuscript Author Manuscript

24. Bland JM, Altman DG. Statistics notes: Calculating correlation coefficients with repeated observations: Part 1--correlation within subjects. BMJ. 1995; 310(6977):446.doi: 10.1136/bmj.310.6977.446 [PubMed: 7873953]
25. Bland JM, Altman DG. Calculating correlation coefficients with repeated observations: Part 2--Correlation between subjects. BMJ. 1995; 310(6980):633. [PubMed: 7703752]
26. Deng M, Griffith JF, Zhu X-M, Poon WS, Ahuja AT, Wang Y-XJ. Effect of ovariectomy on contrast agent diffusion into lumbar intervertebral disc: a dynamic contrast-enhanced MRI study in female rats. Magn Reson Imaging. 2012; 30(5):683–688. DOI: 10.1016/j.mri.2012.01.001 [PubMed: 22459440]
27. Niinimäki JL, Parviainen O, Ruohonen J, et al. In vivo quantification of delayed gadolinium enhancement in the nucleus pulposus of human intervertebral disc. J Magn Reson Imaging. 2006; 24(4):796–800. DOI: 10.1002/jmri.20693 [PubMed: 16929532]
28. Eltoum IA, Siegal GP, Frost AR. Microdissection of histologic sections: past, present, and future. Adv Anat Pathol. 2002; 9(5):316–322. [PubMed: 12195221]
29. Scoazec J-Y. Tissue and cell imaging in situ: potential for applications in pathology and endoscopy. Gut. 2003; 52(suppl 4) iv1 LP-iv6. http://gut.bmj.com/content/52/suppl_4/iv1.abstract.
30. Grunert P, Hudson KD, Macielak MR, et al. Assessment of intervertebral disc degeneration based on quantitative magnetic resonance imaging analysis: an in vivo study. Spine (Phila Pa 1976). 2014; 39(6):E369–78. DOI: 10.1097/BRS.0000000000000194 [PubMed: 24384655]
31. Grunert P, Borde BH, Hudson KD, Macielak MR, Bonassar LJ, Hartl R. Annular repair using high-density collagen gel: a rat-tail in vivo model. Spine (Phila Pa 1976). 2014; 39(3):198–206. DOI: 10.1097/BRS.0000000000000103 [PubMed: 24253790]
32. Brateman L. Chemical shift imaging: a review. Am J Roentgenol. 1986; 146(5):971–980. DOI: 10.2214/ajr.146.5.971 [PubMed: 3008543]
33. Martin JT, Gorth DJ, Beattie EE, Harfe BD, Smith LJ, Elliott DM. Needle puncture injury causes acute and long-term mechanical deficiency in a mouse model of intervertebral disc degeneration. J Orthop Res. 2013; 31(8):1276–1282. DOI: 10.1002/jor.22355 [PubMed: 23553925]
34. Hsieh AH, Hwang D, Ryan DA, Freeman AK, Kim H. Degenerative anular changes induced by puncture are associated with insufficiency of disc biomechanical function. Spine (Phila Pa 1976). 2009; 34(10):998–1005. DOI: 10.1097/BRS.0b013e31819c09c4 [PubMed: 19404174]
35. Castro APG, Paul CPL, Detiger SEL, et al. Long-Term Creep Behavior of the Intervertebral Disk: Comparison between Bioreactor Data and Numerical Results. Front Bioeng Biotechnol. 2014; 2:56.doi: 10.3389/fbioe.2014.00056 [PubMed: 25485264]
36. Casaroli G, Galbusera F, Jonas R, Schlager B, Wilke H-J, Villa T. A novel finite element model of the ovine lumbar intervertebral disc with anisotropic hyperelastic material properties. PLoS One. 2017; 12(5):e0177088.doi: 10.1371/journal.pone.0177088 [PubMed: 28472100]
37. Gu T, Shi Z, Wang C, et al. Human bone morphogenetic protein 7 transfected nucleus pulposus cells delay the degeneration of intervertebral disc in dogs. J Orthop Res. 2017; 35(6):1311–1322. DOI: 10.1002/jor.22995 [PubMed: 26218641]
38. Zhu Q, Gao X, Temple HT, Brown MD, Gu W. Simulation of biological therapies for degenerated intervertebral discs. J Orthop Res. 2016; 34(4):699–708. DOI: 10.1002/jor.23061 [PubMed: 26425965]
39. Hayami S, Ishigooka M, Suzuki Y, Hashimoto T, Nakada T, Mitobe K. Comparison of the nephrotoxicity between ioversol and iohexol. Int Urol Nephrol. 1996; 28(5):615–619. [PubMed: 9061418]
40. Liu JW, Lin KH, Weber C, et al. An In Vitro Organ Culture Model of the Murine. Intervertebral Disc. 2017; (122):e55437.doi: 10.3791/55437

Author Manuscript Author Manuscript Author Manuscript Author Manuscript

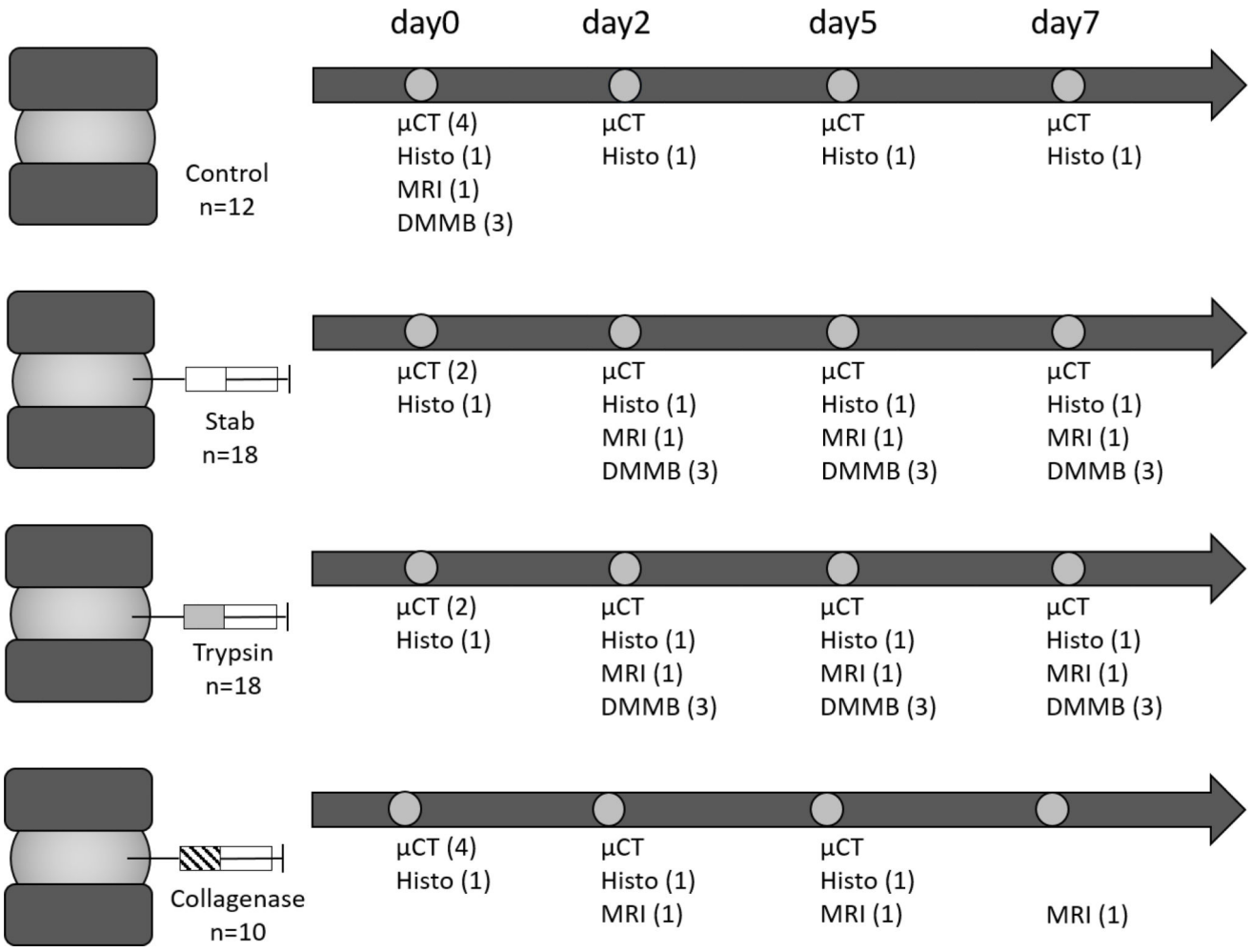

Figure 1.

Experimental design and workflow detailing the distribution of samples and imaging and assay modalities used. A total of 44 rat FSUs were used in this study with n = 10–12 per treatment group. µCT = contrast-enhanced microCT using Ioversol; Histo= histology by Safranin-O/Fast Green; MRI = Magnetic resonance imaging; DMMB = Dimethylmethylene Blue Assay.

Author Manuscript Author Manuscript Author Manuscript Author Manuscript

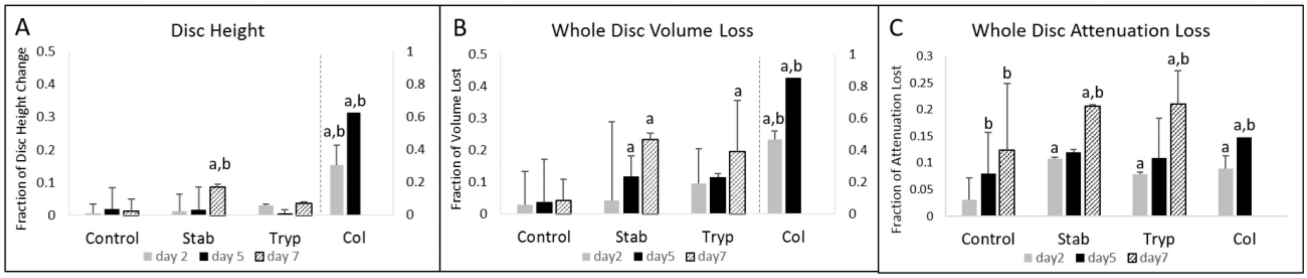

Figure 2.

Longitudinal quantitation by contrast-enhanced microCT revealed that changes of the IVD structure as a result of the stab- , trypsin-, and collagenase- administration. The treatment ($p < 0.05$) and incubation duration ($p < 0.01$) were significant factors that altered the change of disc height (Panel A; ANOVA), whole disc volume loss (Panel B; $p < 0.01$ [treatment]; $p < 0.01$ [incubation duration]; ANOVA), and whole disc attenuation loss (Panel C; $p < 0.001$ [treatment]; $p < 0.001$ [incubation duration]; ANOVA). In each of these factors, treatment and incubation time had an interactive effect that significantly contributed to these changes with $p < 0.05$ in all measurements. a - denotes $p < 0.05$ compared with the control group of the same incubation time. b - denotes $p < 0.05$ compared with the same treatment at zero day.

Author Manuscript
Author Manuscript
Author Manuscript
Author Manuscript

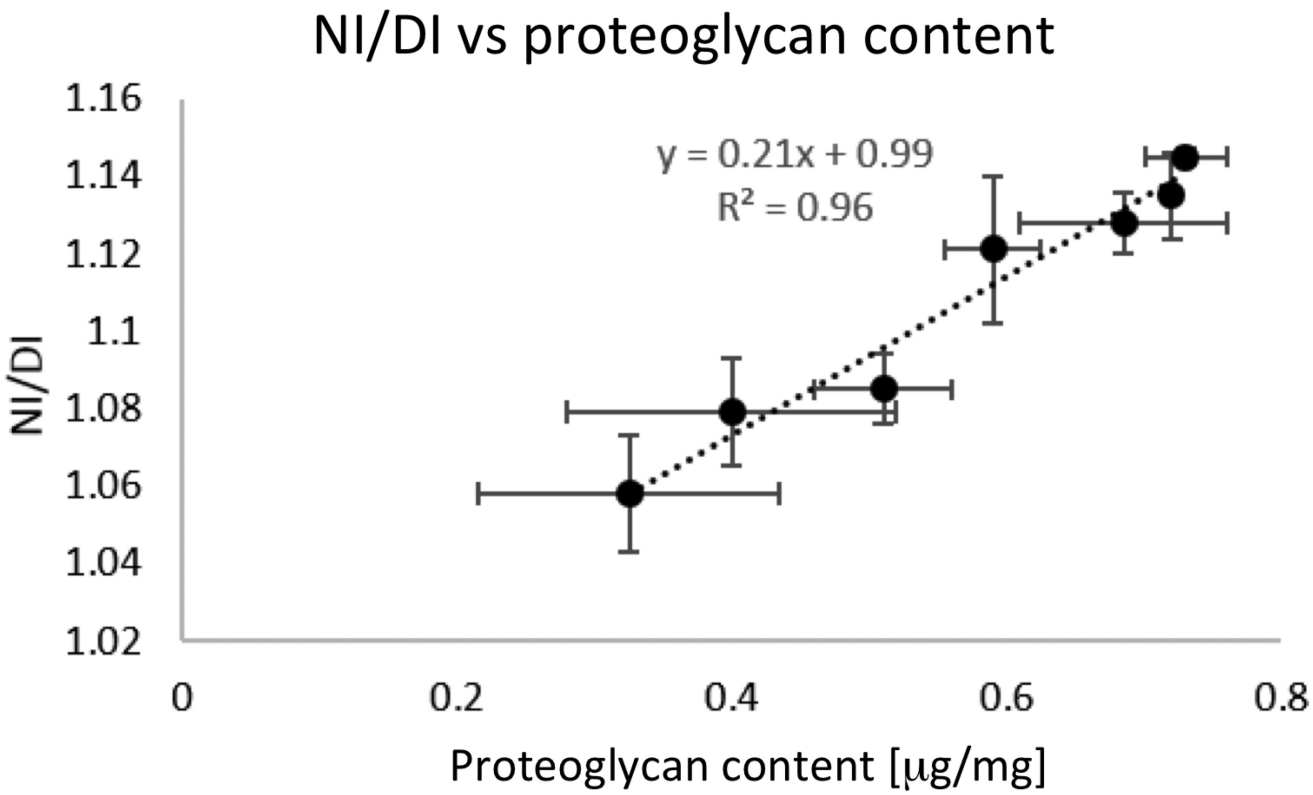

Figure 3.

Nucleus pulposus intensity to whole disc intensity (NI/DI) was computed for the control, stab-, and trypsin- samples. The DMMB assay, normalized to chondroitin sulfate, was conducted on these samples following microCT. The NI/DI was significantly and highly correlated with the proteoglycan composition of the disc ($p < 0.001$; $r^2 = 0.9581$; Pearson's correlation).

Author Manuscript Author Manuscript Author Manuscript Author Manuscript

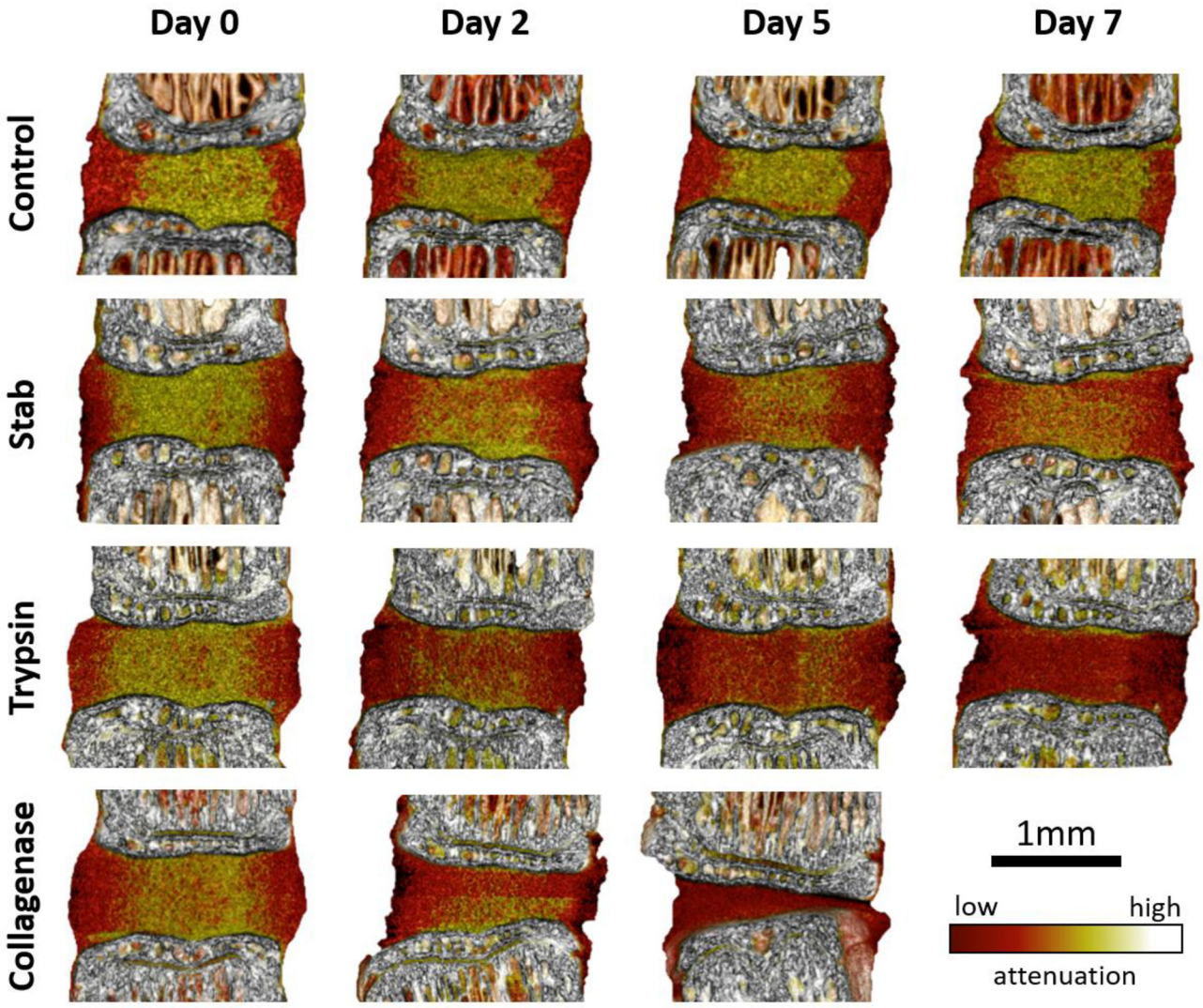

Figure 4.

Contrast-enhanced microCT can monitor the progressive degenerative changes in stab-, trypsin-, and collagenase- degeneration models. These changes can be monitored longitudinally, and enables the ability to quantify localized and nuanced changes within the IVD. The control samples showed clear presentation of the NP, while the stab- and trypsin-degeneration groups revealed a progressive loss of the NP attenuation. The collagenase samples show an immediate loss of the NP and collapse of the AF.

Author Manuscript Author Manuscript Author Manuscript Author Manuscript

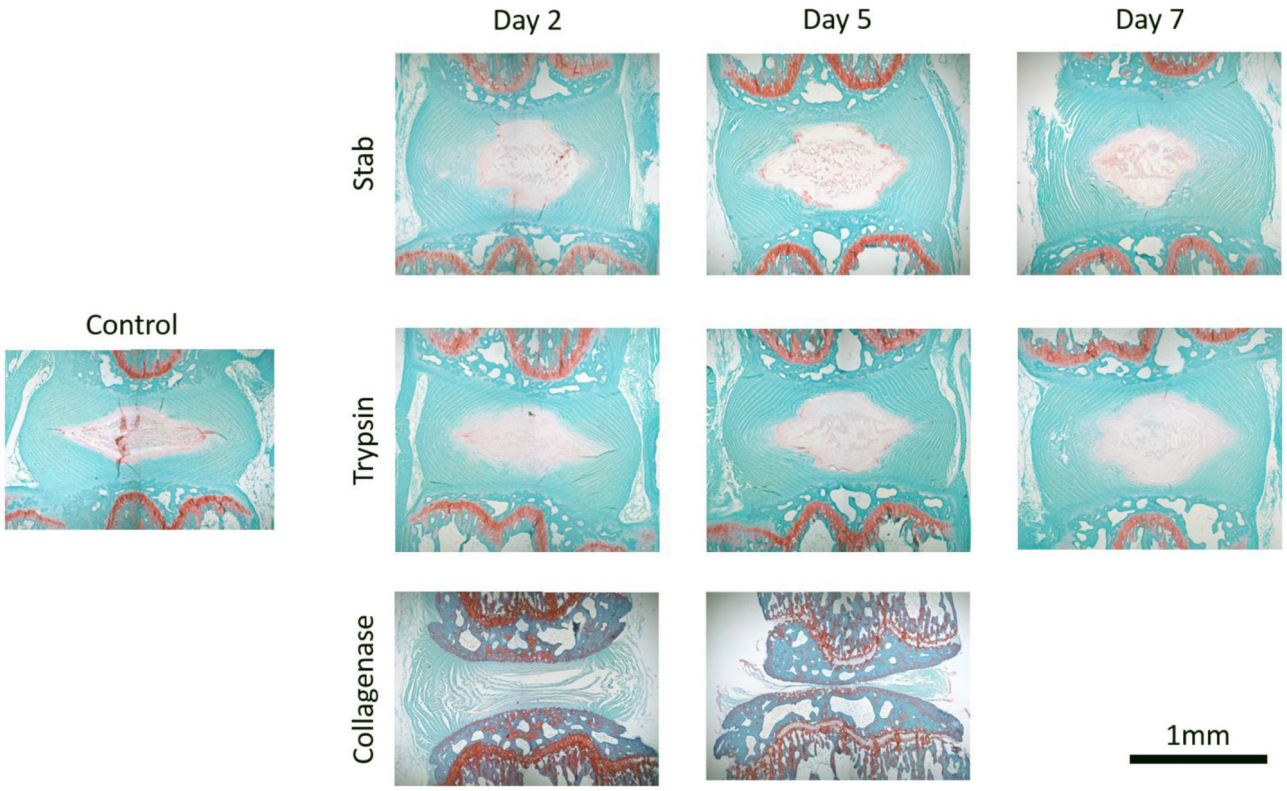

Figure 5.

Histology samples show similar patterns of degradation observed from the microCT imaging. Although each histological image is taken from a different sample and thus cannot be directly compared longitudinally, the appears to be a general trend with the stab and trypsin samples showing decreased intensity of Saf-O staining in the NP when compared to the control sample. Collagenase treated samples show complete loss of the NP by day 2 and complete breakdown of the disc structure by day 5. Collagenase also affects the entire tissue, which is apparent by the altered dye intake of the collagenase samples with histology.

Author Manuscript Author Manuscript Author Manuscript Author Manuscript

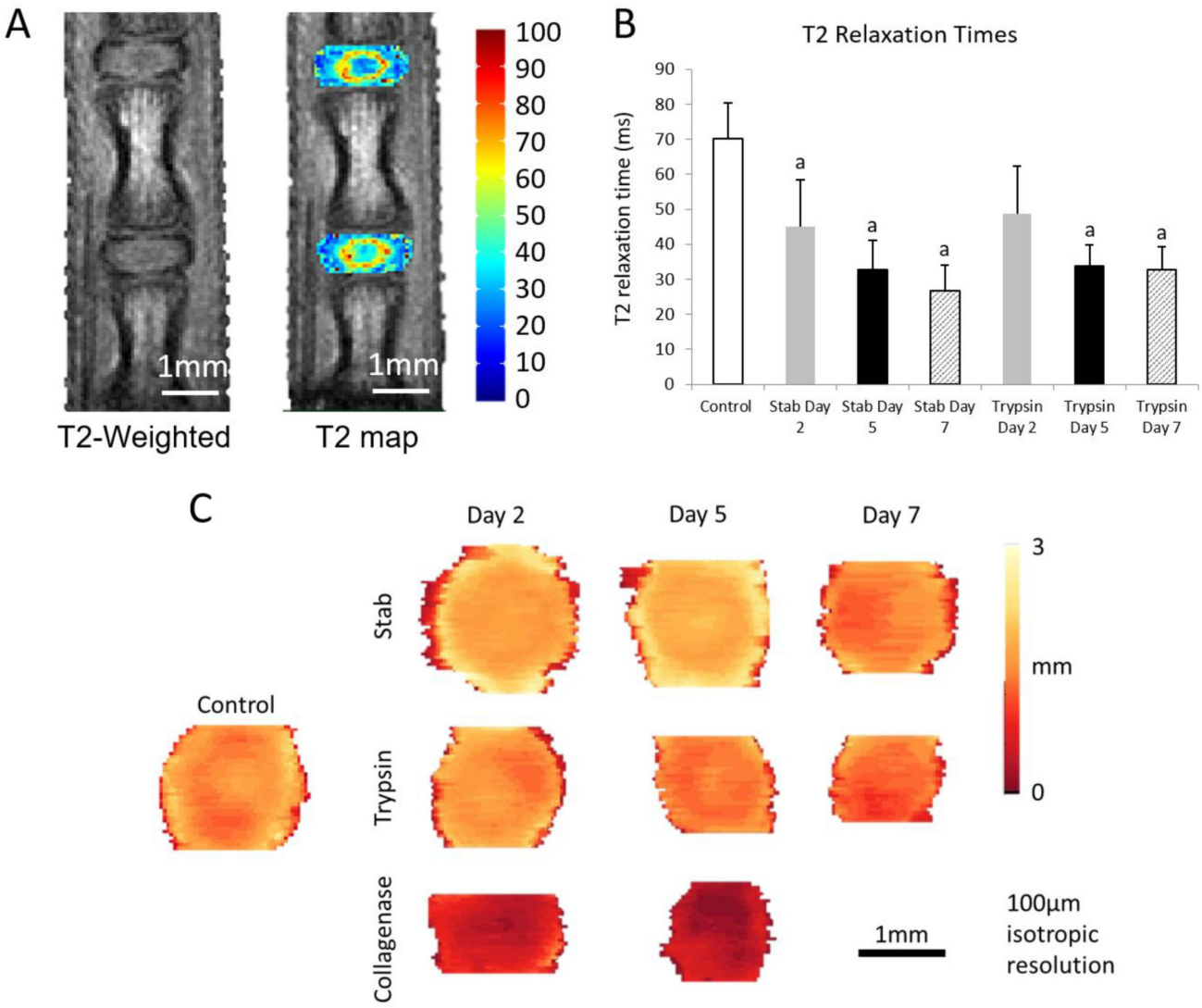

Figure 6.

(A) T2 weighted imaging and T2 relaxation mapping were conducted on the control, stab-, trypsin, and collagenase- groups. (B) The distribution of T2 relaxation times confirm a significant reduction of T2 times due to degeneration. a - denotes $p < 0.05$ compared with the control group. (C) The transverse thickness map of the IVD show a loss of the disc thickness as well as the disc area across the degeneration models over time.